International Journal of Mass Spectrometry 369 (2014) 30–35

Contents lists available at ScienceDirect

International Journal of Mass Spectrometry

journal homepage: www.elsevier.com/locate/ijms

Optimized DLP linear ion trap for a portable non-scanning mass spectrometer

Boris Brkić [a,*], Stamatios Giannoukos [a], Neil France [b], Robert Murcott [c], Fabrizio Siviero [d], Stephen Taylor [a]

[a] Department of Electrical Engineering and Electronics, University of Liverpool, Brownlow Hill, Liverpool L69 3GJ, United Kingdom
[b] Q Technologies Ltd, 100 Childwall Road, Liverpool L15 6UX, United Kingdom
[c] TWI Technology Centre Yorkshire, Advanced Manufacturing Park, Wallis Way, Catcliffe, Rotherham S60 5TZ, United Kingdom
[d] Vacuum Technology Lab, SAES Getters S.p.A., Viale Italia 77, Lainate 20020, Milan, Italy

ARTICLE INFO

Article history:
Received 7 April 2014
Received in revised form 23 May 2014
Accepted 2 June 2014
Available online 4 June 2014

Keywords:
Linear ion trap
Rapid prototyping
Portable mass spectrometer
Non-scanning mode
Security applications

ABSTRACT

This work reports implementation of an optimized linear ion trap (LIT) mass analyzer manufactured using digital light processing (DLP), a low cost rapid prototyping technique. To satisfy requirements for a portable commercial instrument, our previous DLP LIT has been improved by using polymer material for electrodes and housing with higher heat deflection temperature and much improved metal coating of the electrodes. In this way, a polymer-based LIT can operate at higher pressures with more stable voltages, low outgassing and with much longer electrode lifetime. This paper demonstrates non-scanning operation of a DLP LIT based on ceramic resin with specially electroplated electrodes. Non-scanning mode is suitable for applications in which only specific mass fragments are targeted such as security and forensics. Experimental results from a DLP LIT are therefore shown for simulants of cocaine, TNT and sarin.

1. Introduction

For in-field applications that require analysis of specific molecules, simple and low cost portable mass spectrometers are highly suitable. Such applications can be found within environmental [1], space exploration [2], automotive [3], medical [4], food [5] and security [6] sectors. When analysis of application-targeted molecules is required, the use of a non-scanning mass spectrometer is highly recommended. This is because a non-scanning mass spectrometer performs selective ion monitoring with optimal voltages for each ion mass without having to obtain full mass spectrum [7,8]. A result of such operation mode is higher sensitivity, simpler control electronics, smaller size, lower power consumption and cost.

Apart from simplicity and cost savings with electronics for a non-scanning mass spectrometer, manufacturing of mass analyzers can also be simplified at significantly lower cost than with conventional techniques. Our previous work has demonstrated design, fabrication and proof of concept for using digital light processing (DLP) technique to implement polymer-based quadrupole mass filter (QMF) [9] and linear ion trap (LIT) [10] with hyperbolic rods. DLP is a rapid prototyping (RP) technique that uses dynamic masking capability to selectively cure a photosensitive polymer resin, which enables fabrication of complicated 3D structures. Modern DLP machines also have enhanced resolution mode (ERM) that further improves surface quality and can provide surface roughness at higher nanoscale levels. Compared to selective laser ablation (SLA), another RP technique used for polymer-based rectilinear ion traps [11–13], DLP provides better manufacturing accuracy and surface smoothness. This is because DLP has much smaller volumetric pixels ($\approx$15 μm × 15 μm ×25 μm) compared to SLA tracks width ($\approx$200 μm) and ERM capability for improving surface quality. Typical arithmetic average (R_a) for surface roughness of DLP parts with 25 μm voxel size is 749 nm with ERM off and 434 nm with ERM on [10]. Due to these advantages, our work has focused on rapid manufacturing of analyzers with hyperbolic electrodes that provide the ideal quadrupole electric field and therefore optimal performance of an analyzer [14,15].

Our previous DLP QMF and LIT were made using polymethylmethacrylate (PMMA), which gave accurate and smooth electrodes. However, some level of outgassing under vacuum was noticed during previous QMF tests from PMMA [9], which resulted in an unwanted pressure increase. For those ion traps that operate at

* Corresponding author. Tel.: +44 151 794 4541; fax: +44 151 794 4540.
E-mail address: Boris.Brkic@liv.ac.uk (B. Brkić).

http://dx.doi.org/10.1016/j.ijms.2014.06.004
1387-3806/

higher pressures than quadrupole mass spectrometers and use buffer gas for ion cooling, outgassing could be further increased and affect mass analysis. Therefore, PMMA has been replaced with ceramic-filled resin (HTM140), which has higher heat deflection temperature (HDT) and lower outgassing rate. The HDT for HTM140 is 140 °C straight out of the machine without performing any UV and thermal post cure processes that would increase it further, while it is 75 °C for PMMA [16]. Another important issue for a polymer-based analyzer is high quality of metal coating on electrodes, which is essential for a commercial instrument. Types of coating used on previous analyzer prototypes are evaporative and sputter processes that deposit gold directly on polymer electrodes [9,10]. Even though such coatings provided very good conductivity on the rods, gold deposits would start to wear out over time on all of our previously made samples. This affects dielectric constant and capacitance between the RF rods, which could cause instability of RF voltages and errors in mass analysis. For these reasons, polymer electrodes were coated using specially adapted electroplating process for plastic structures. Coating included thick base layer of copper and nickel with thin layer of high gloss gold, which provided very firm attachment of metal layers to the rods and excellent electrical conductivity.

The following section describes experimental characteristics of a non-scanning LIT, DLP machining, electroplating process and experimental setup for tests with a non-scanning DLP LIT. Results and discussion are given for optimized DLP LIT prototype, outgassing tests with HTM140 polymer, and experiments with DLP LIT for detection of key mass fragments in simulants for cocaine, TNT and sarin.

2. Experimental

2.1. Non-scanning linear ion trap

Theory of a non-scanning LIT has been described in detail by Brkić et al. [8]. In a non-scanning mode, only one specific targeted ion mass is confined within an analyzer and ejected at a time. Mass isolation is performed by applying suitable RF and DC voltages on LIT rods with values near the tip of the stability diagram for given ion mass. Fig. 1 shows a schematic diagram of a non-scanning LIT consisting of four hyperbolic rod electrodes for radial (x,y) ion confinement and two disc endcap electrodes for axial (z) confinement. Positive ions are radially trapped and isolated by applying constant positive RF and DC voltages to y-axis rods (y-electrodes) and negative DC voltage to x-axis rods (x-electrodes). Axial confinement is done by applying identical positive DC voltages to entrance and exit endcaps (z-electrodes). Our LIT is designed for axial ion injection and ejection, which are done through the holes on entrance and exit endcaps respectively. During ion injection, entrance endcap is switched to zero or low DC to allow ions to enter the trap, while during ejection exit endcap is switched to negative DC to extract the ions from the trap.

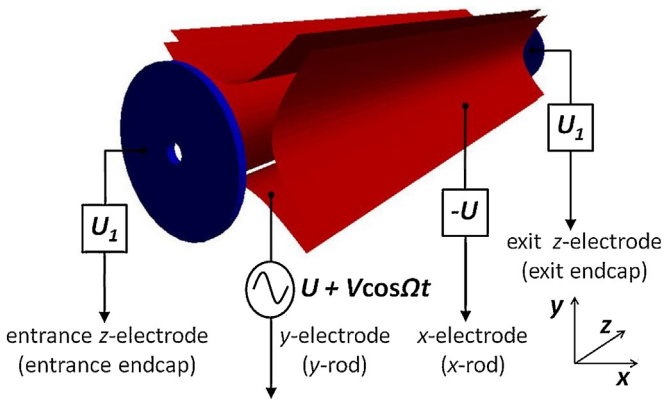

Fig. 1. Schematic diagram of a non-scanning hyperbolic linear ion trap.

2.2. DLP machining

Typical fabrication procedure in a DLP machine consists of the following steps:

(a) CAD model is loaded into a machine and processed using its software,
(b) Model is vertically sliced into a series of individual layers of 25 μm thickness,
(c) Direct light projector projects a mask of the slice to be processed using a digital micromirror device (DMD),
(d) Build substrate moves up by 25 μm,
(e) Procedure is repeated until all slices are processed.

The DLP machine used for LIT manufacturing is Envisiontec Perfactory 3 Mini Multi Lens with ERM. It uses 700 mW/dm^2 of visible light at 25 μm layers. Smallest ERM voxel size is 16 μm. Maximum build envelope available is 84 mm × 63 mm × 230 mm. The build time of structures is not dependent on the number/size of parts, but only on the height of the parts. Manufacture of multiple DLP LIT parts takes approximately 11 h.

2.3. Electroplating process

The Metalise™ process from 3DDC Ltd, UK was used for the metallic coating of DLP LIT rod electrodes. This method has been specifically developed for plastic components that have been produced via additive manufacturing. The DLP electrodes were initially pre-processed using a fine sanding procedure. The surface roughness of the parts was previously reduced using ERM capability to allow for the electroplating process to be carried out and to achieve the best operational results. This is because patch potentials on rough areas of LIT electrodes could increase ion motional heating, which would cause distortion of ion motion [17]. For the LIT electrode application, a thick layer of copper and nickel (130 μm) was first applied before the final coating with high gloss gold (0.3 μm). The hyperbolic outer surfaces of the electrodes were then polished smooth for best performance. This coating technique is a specially adapted electroplating process, where electrical current is applied to an anode and cathode both placed into an electrolytic solution. In this case, the cathode is the DLP electrode and the anode would be either a sacrificial anode or an inert anode. Material is transferred from the anode to the cathode and over time the cathode is plated. The process is summarized in Fig. 2.

2.4. Experimental setup

Experiments with DLP LIT were performed using Pfeiffer's miniature vacuum system consisting of diaphragm pump MVP 006-4 with 6 l/min pumping speed and turbomolecular pump HiPace 10 with 10 l/s pumping speed. The system provides base pressure of 5×10^{-6} Torr with a small spectrometer chamber connected to it. Test sample vapors were injected into the vacuum system using membrane inlet assembled in a 1/4 in. Swagelok fitting union with 0.12 mm SIL-TEC sheet membrane. DLP LIT was assembled with in-house made electron impact (EI) ion source with a three-lens system and dual thoria filaments, and channeltron type electron multiplier detector (Photonis, US). The whole LIT spectrometer was assembled on a CF40 vacuum flange. Data acquisition was performed with in-house built PCB-

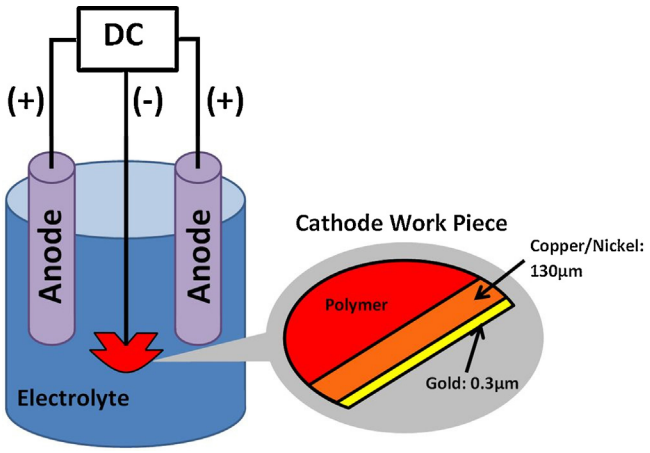

Fig. 2. Schematic diagram of electroplating process used for enhanced coating of DLP linear ion trap.

based electronics closely coupled to the flange with operational power consumption of 34 W.

3. Results and discussion

3.1. Fabrication

For accurate alignment and fitting of DLP LIT electrodes, a stack of rods and housings were designed and fabricated with different tolerances for choosing the right match. Fig. 3a shows defined geometries for rods and housings on a build envelope of the DLP machine with slightly different groove dimensions for different tolerances. Compared to conventional methods, this method is fast and cost effective for obtaining desired inter-electrode distance ($2r_0$) and alignment. As can be seen in Fig. 3b, grooves in housing for the rods are made slightly larger to accommodate electroplated rods with thick coating and maintain their separation. Top part of the housing has its outer diameter slightly reduced to accommodate base holder for entrance endcap and ion source. The bottom part of the housing has its diameter adjusted to the size of insulating adaptor, which provides separation between the exit endcap and multiplier shielding tube. The length of DLP LIT rods is 40 mm with 2.5 mm r_0. Endcaps are 0.4 mm thick discs separated from the rods by 0.8 mm with 1.5 mm aperture radius. Due to low manufacturing costs for simple disc electrodes, endcaps are made from stainless steel using conventional manual machining, while DLP is kept for complicated electrode shapes and isolation parts. Fig. 3c shows high quality electroplated LIT rods with thick layer of copper/nickel (130 μm) and thin layer of gold (0.3 μm). Rods are slid into the housing with a tight fit and additionally supported with miniature screws for electrical contact for which holes are made in the housing. Resistance on electroplated DLP rods from top to bottom is less than 0.01 Ω. Measured capacitance between x and y-electrodes is 13.6 pF.

3.2. Outgassing

Outgassing molecules from polymer resin materials mainly include water vapors and atmospheric gases [18]. The outgassing levels of these molecules could change with different surrounding temperatures. Since the housing of the DLP LIT is always exposed to some level of heat (e.g. radiated from vacuum system or EI ion source), outgassing tests were performed with a DLP sample in a heated chamber with a separate vacuum system. Tests were done at 50 and 100 °C temperatures, even though 100 °C is higher than the temperature to which DLP LIT is exposed during operation.

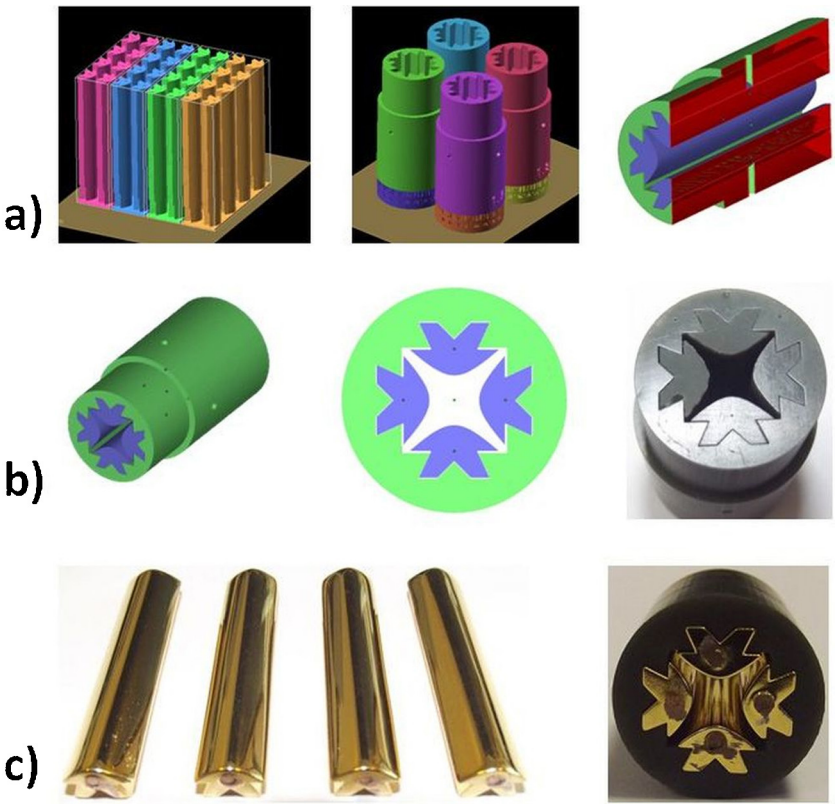

Fig. 3. Design, fabrication and assembly of DLP linear ion trap: (a) fabrication design stack of DLP LIT rods and housings on a machine build envelope with vertical cross section of LIT assembly, (b) fabrication design of LIT assembly with non-coated prototype, (c) electroplated LIT rods and final rod assembly in ceramic resin housing.

Table 1
Outgassing tests with HTM140 material at 50 and 100 °C temperatures.

	Gas presence after 30 min of degassing at 50 °C (ccmbar)	Gas presence after 30 min of degassing at 100 °C (ccmbar)	Gas presence after 30 min of degassing at 50 °C (%)	Gas presence after 30 min of degassing at 100 °C (%)
H_2	4.6E-05	6.3E-04	0.79	1.15
He	0	0	0	0
CO	0	0	0	0
N_2	3.8E-03	3.4E-02	65.55	63.51
CH_4	1.5E-05	2.5E-04	0.27	0.47
H_2O	0	0	0	0
O_2	6.0E-08	1.5E-06	0	0
Ar	7.1E-05	5.5E-04	1.23	1.02
CO_2	1.9E-03	1.8E-02	32.16	33.85
Kr	0	0	0	0
Total	5.8E-03	5.4E-02	100	100

Table 1 shows outgassing levels of typical air gases when HTM140 material is exposed to heat. Results are for a chamber with HTM140 after 30 min of degassing at 50 and 100 °C. Gas levels were measured using a single filter quadrupole mass spectrometer and for each molecule they are shown in ccmbar and in relative percentages. After temperature exposure, no water levels were seen and very low levels of hydrogen were present. As expected, nitrogen and carbon dioxide were the most abundant gases with argon and methane present in low amounts. No traces of helium, carbon monoxide, oxygen and krypton were seen after temperature degassing. It can be seen that there are minor differences between degassing of air molecules for 50 and 100 °C temperatures. In a miniature Pfeiffer's system used for LIT mass analysis, only a small rise in base pressure was seen with HTM140 LIT inside. Pressure went up from 5×10^{-6} Torr with a blank chamber to 7×10^{-6} Torr with HTM140 LIT present. On the other hand, base pressure with PMMA LIT went up to 2×10^{-5} Torr, which shows more significant outgassing and less room for adding sample and buffer gas. Therefore, in terms of analyzer sensitivity, overall operation and usage in a commercial system, HTM140 is a better choice than PMMA.

3.3. Experiments

After non-scanning DLP LIT mass spectrometer has been assembled, tuned and calibrated, it was tested with simulants for cocaine, TNT and sarin, which are respectively methyl benzoate (Fisher Scientific Ltd, UK), 2-nitrotoluene (Sigma Aldrich Co. LLC., UK) and dimethyl methylphosphonate (Sigma-Aldrich Co. LLC., UK). Since all the samples were in a liquid form, they were prepared in 1 l flasks by injecting drops from the micropipetter (Brand GmbH, Germany). Concentrations of 5 ppm were made for each sample by injecting required drop size into a flask, covering flask top with several layers of parafilm and leaving the sample at room temperature for 3 h to reach equilibrium. The required drop sizes for 5 ppm of methyl benzoate, 2-nitrotoluene and dimethyl methylphosphonate were 7.6, 7.75 and 7.01 μL respectively. After preparation, sheet membrane inlet connected to the vacuum system was inserted into the flask through parafilm to perform sample analysis. In this way, volatile organic compounds (VOCs) from sample vapors would enter the vacuum system through the pores of a sheet membrane. The vacuum system pressure was initially at 1×10^{-5} Torr with the sample inlet valve fully open and it was increased to 8×10^{-5} Torr after adding helium buffer gas for ion cooling and sensitivity enhancement.

The mass analysis cycle for individual mass fragments included following steps: ionisation/ion injection (10 ms), ion trapping (1 ms), mass selection (1 ms) and ion ejection (10 ms). An EI ion source provided 100 μA electron emission current with 1.73 A filament current. The EI source electron repeller was held at −20 V, ion cage at 3 V, ion focusing lens at −100 V and ion deceleration lens at zero. LIT entrance endcap was held at 20 V and switched to zero during ion injection. Exit endap was at 20 V and switched to −100 V during ion ejection. The LIT was driven at 985 kHz RF frequency and RF voltage on *y*-rods was set for each ion mass and kept constant during the whole analysis cycle. Negative and

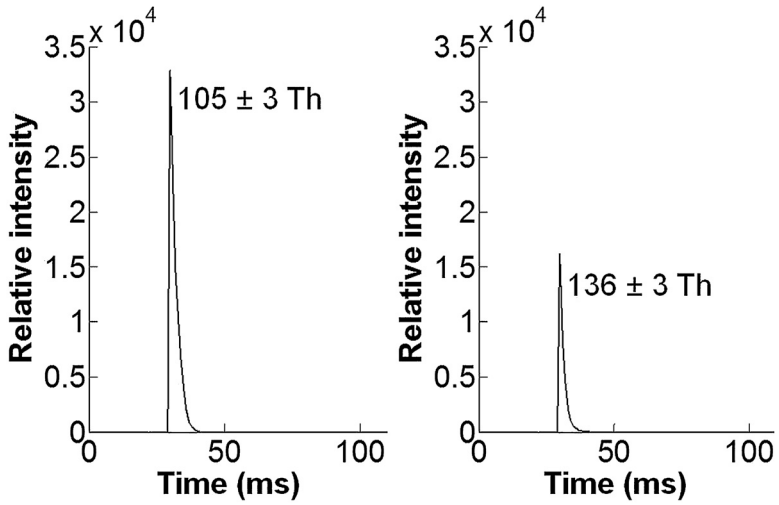

Fig. 4. Key experimental mass fragments for 5 ppm methyl benzoate (cocaine simulant) obtained from the non-scanning DLP LIT.

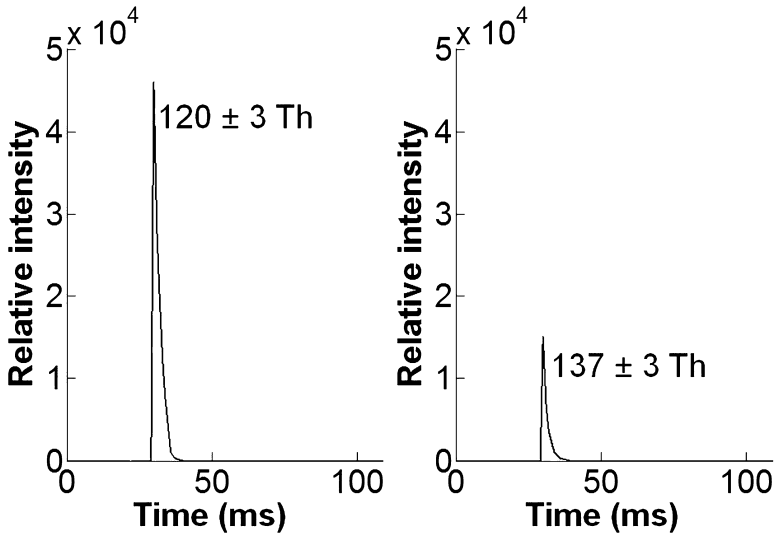

Fig. 5. Key experimental mass fragments for 5 ppm 2-nitrotoluene (TNT simulant) obtained from the non-scanning DLP LIT.

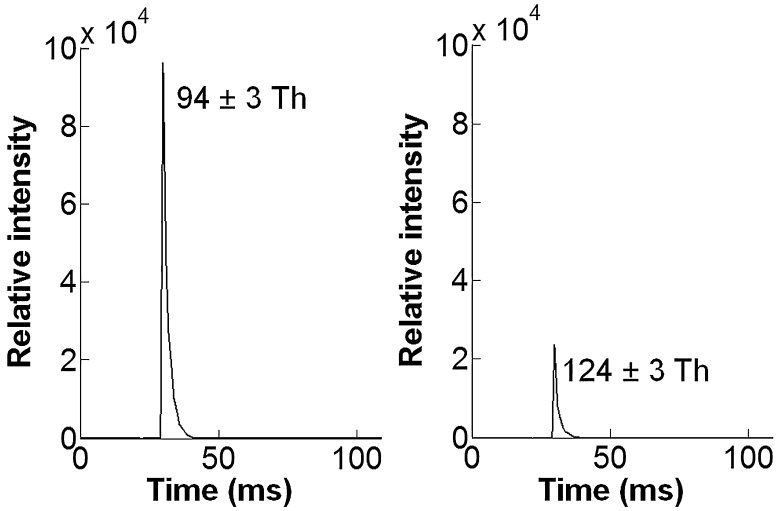

Fig. 6. Key experimental mass fragments for 5 ppm dimethyl methylphosphonate (sarin simulant) obtained from the non-scanning DLP LIT.

positive DC pulses were applied to *x* and *y*-rods respectively only during mass selection to set mass window width. The electron multiplier was held at −1200 V for analysis of all samples.

Figs. 4–6 show key experimental mass fragments for methyl benzoate, 2-nitrotoluene and dimethyl methylphosphonate obtained from the non-scanning DLP LIT. The chosen mass fragments represent most abundant mass peaks and molecular masses for each compound. The RF and DC voltages used for isolation of each mass fragment are the following:

- methyl benzoate: 188 Vp-p RF and ±7.9 V DC for $m/z > 105$; 244 Vp-p RF and ±10.2 V DC for $m/z > 136$,
- 2-nitrotoluene: 216 Vp-p RF and ±9 V DC for $m/z > 120$; 246 Vp-p RF and ±10.3 V DC for $m/z > 137$,
- dimethyl methylphosphonate: 170 Vp-p RF and ±7.1 V DC for $m/z > 94$; 222 Vp-p RF and ±9.3 V DC for $m/z > 124$.

The mass window width obtained for each fragment peak was 6 Th, keeping RF/DC ratio constant for each mass. Upper and lower limits of the mass window were determined by increasing RF/DC voltages at same ratio until the mass peak disappeared. With fine adjustments and small alteration of RF/DC ratio, 4 Th width could be achieved. Our simulation results have also shown that a swift DC ramp on the rods (in μs) within small DC range can filter out adjacent masses and possibly allow unit resolution for this type of non-scanning LIT [19]. This could significantly increase the number of applications for a simple and low cost mass spectrometer.

4. Conclusions

This paper has demonstrated optimization of a polymer-based non-scanning LIT fabricated using DLP rapid prototyping technique. Usage of ceramic resin material for making LIT rod electrodes and electrode housing has minimized outgassing, while specialized electroplating of the rods with copper, nickel and gold has provided very firm coating with longer electrode life. With such optimization, DLP LIT has been made more suitable for a commercial system. Experimental results for cocaine, TNT and sarin simulants are shown for enhanced DLP LIT operating in a non-scanning mode with simplified control electronics. Such

simplification and cost reduction of a mass analyzer and electronics provide a good basis for a portable application-specific mass spectrometer.

Acknowledgements

The research leading to these results has received funding from the European Community's Seventh Framework Programme managed by REA Research Executive Agency (FP7/2007–2013) under grant agreement no. 285045. We thank our project partners Aix Marseille University, Da Vinci Laboratory Solutions, Envisiontec GbmH, XaarJet AB and Wagtail UK Ltd. The author greatly thanks Tom Hogan from Pathway Systems and Ray Gibson from University of Liverpool for their technical assistance.

References

[1] B. Brkić, N. France, S. Taylor, Anal. Chem. 83 (2011) 6230.
[2] P.T. Palmer, T.F. Limero, J. Am. Soc. Mass Spectrom. 12 (2001) 656.
[3] P. Kusch, V. Obst, D. Schroeder-Obst, W. Fink, G. Knupp, J. Steinhaus, Eng. Fail. Anal. 35 (2013) 114.
[4] P. Nemes, A. Vertes, Trends Anal. Chem. 34 (2012) 22.
[5] S. Soparawalla, F.K. Tadjimukhamedov, J.S. Wiley, Z. Ouyang, R.G. Cooks, Analyst 136 (2011) 4392.
[6] P.I. Hendricks, J.K. Dalgleish, J.T. Shelley, M.A. Kirleis, M.T. McNicholas, L. Li, T.C. Chen, C.H. Chen, J.S. Duncan, F. Boudreau, R.J. Noll, J.P. Denton, T.A. Roach, Z. Ouyang, R.G. Cooks, Anal. Chem. 86 (2014) 2900.
[7] C. Zhang, H. Chen, A.J. Guymon, G. Wu, R.G. Cooks, Z. Ouyang, Int. J. Mass spectrom. 1 (2006) 225–256.
[8] B. Brkić, S. Giannoukos, N. France, A. Janulyte, Y. Zerega, S. Taylor, Int. J. Mass Spectrom. 353 (2013) 36.
[9] B. Brkić, N. France, A.T. Clare, C.J. Sutcliffe, P.R. Chalker, S. Taylor, J. Am. Soc. Mass Spectrom. 20 (2009) 1359.
[10] A.T. Clare, L. Gao, B. Brkić, P.R. Chalker, S. Taylor, J. Am. Soc. Mass Spectrom. 21 (2010) 317.
[11] M. Fico, M. Yu, Z. Ouyang, R.G. Cooks, W.J. Chappell, Anal. Chem. 79 (2007) 8076.
[12] M. Fico, J.D. Maas, S.A. Smith, A.B. Costa, Z. Ouyang, W.J. Chappell, R.G. Cooks, Analyst 134 (2009) 1338.
[13] J.D. Maas, P.I. Hendricks, Z. Ouyang, R.G. Cooks, W.J. Chappell, IEEE J. Microelectromech. Syst. 19 (2010) 951.
[14] W.M. Brubaker, W.S. Chamberlin, Proceedings of the international conference on mass spectroscopy, University Park Press, Baltimore, MD, 981970).
[15] J.R. Gibson, S. Taylor, Rapid Commun. Mass Spectrom. 14 (2000) 1669.
[16] PMMA data sheet available from Envisiontec GmbH, www.envisiontec.com
[17] Q.A. Turchette, D. Kielpinski, B.E. King, D. Leibfried, D.M. Meekhof, C.J. Myatt, M.A. Rowe, C.A. Sackett, C.S. Woods, W.M. Itano, C. Monroe, D.J. Wineland, Phys. Rev. A 61 (2000) 063418.
[18] R.D. Brown, Vacuum 17 (1967) 505.
[19] K.G. Evans and J.R. Gibson, University of Liverpool, private communication